Molecular Vision 2025; 31:175-188 <http://www.molvis.org/molvis/v31/175>
Received 7 December 2024 | Accepted 14 May 2025 | Published 16 May 2025

Mutation of beta-tubulin 4B gene (*TUBB4B)* causes autosomal dominant retinitis pigmentosa with sensorineural hearing loss in a multigenerational family

Cheryl Y. Gregory-Evans,[1] Aaron W. Joe,[2] Kevin Gregory-Evans[1]

[1]Department of Ophthalmology and Visual Sciences, University of British Columbia, Vancouver, Canada; [2]Kelowna General Hospital, British Columbia, Canada

Purpose: Members of a multigenerational Canadian family presented to an inherited retinal degeneration (IRD) clinic with retinitis pigmentosa (RP) and sensorineural hearing loss, reminiscent of an Usher syndrome phenotype. Biallelic disease-causing variants in the known Usher syndrome genes were not identified. Therefore, we enrolled further family members in this study and examined whether other IRD gene variants could explain the phenotype in the family.
Methods: Family members underwent a comprehensive ophthalmic examination, including best-corrected visual acuity, direct and indirect ophthalmoscopy, fundus photography, visual field testing, spectral-domain optical coherence tomography, audiological examination, and genetic testing. Some patients also had autofluorescence imaging. Loss-of-function testing was initiated by antisense morpholino knockdown of *tubb4b* in zebrafish.
Results: Multimodal clinical testing in affected patients revealed an autosomal dominant late-onset presentation of RP associated with progressive, bilateral sensorineural hearing loss that occurred in the second to third decades of life with no vestibular involvement. Panel-based genetic testing revealed a heterozygous c.1168C>T, p.Arg390Trp variant in the beta-tubulin 4B gene (*TUBB4B*) only in affected family members. Based on *in silico* analysis, segregation analysis through the family, and literature evaluation, this variant is likely to be the disease-causing variant inherited in an autosomal dominant manner. We searched our local database of ~1,000 patients with IRD, and no other *TUBB4B* variants were identified, confirming this is a rare disease variant. Knockdown of *tubb4b* in zebrafish revealed cone and rod photoreceptor abnormalities in the retina and hydrocephalus in the developing brain, resulting in early larval lethality.
Conclusions: For the first time, we describe a multigenerational family with a *TUBB4B* gene variant p.(Arg390Trp) segregating with deaf-blindness, establishing autosomal dominant inheritance. This further confirms that the Arg390 codon is a mutation hotspot. We also expand the range of phenotypes seen with the p.(Arg390Trp) *TUBB4B* gene variant to include typical RP as well as a milder, pericentral RP. Furthermore, our studies suggest there is conservation of TUBB4B ciliary function between zebrafish and humans, making zebrafish a better model system for studying vision loss than the mouse model.

Varying degrees of vision loss associated with hearing deficits occur in a highly heterogeneous group of conditions caused by genetic defects, infections, and autoimmune diseases [1-3]. Genetic causes often present from birth to early adulthood in conditions that affect primary cilia, including Usher [4], Bardet-Biedl [5], CHARGE [6], Waardenburg [7], Stickler [8], and Alstrom [9] syndromes. The most commonly seen is Usher syndrome, with a prevalence of between 4 and 17 cases per 100,000 individuals, and accounts for about 50% of all hereditary deaf-blindness cases [10,11], but in pediatric populations, the prevalence is relatively higher at ~1:6,000 [12]. Usher syndrome is characterized by the dual phenotype of sensorineural hearing loss and progressive retinitis pigmentosa (RP), with or without vestibular defects [11,13]. To date, Usher syndrome is known to be caused by defects in 13 genes (RetNet) and is usually inherited in an autosomal recessive manner, although a rare form of the phenotype occurs due to digenic inheritance of mutations in *PDZD7* and *MYO7A* [14].

Four types of Usher syndrome differ based on age of onset, severity of hearing loss, and presence of vestibular involvement (see OMIM 618144). Usher type 1 is the most severe form of the disease, characterized by profound sensorineural hearing loss at birth, abnormal vestibular function, and prepubertal onset of RP [4]. Night blindness and loss of visual fields rapidly progress to registrable blindness by the third decade of life [15]. Usher type 2 (USH2) is the most common subtype, with a congenital mild-to-moderate sensorineural hearing loss, normal vestibular function, and RP that is usually diagnosed in the second decade of life [16]. Usher type 3 accounts for 2% to 4% of cases displaying postlingual

Correspondence to: Cheryl Gregory-Evans, Department of Ophthalmology and Visual Sciences, University of British Columbia, 2550 Willow Street, Vancouver, BC, V5Z 3N9, Canada; Phone: 1-778-968-4349; FAX: 1-604-675-3010; email: cge30@mail.ubc.ca

sensorineural hearing loss that can progress to profound deafness [17,18]. Vestibular dysfunction occurs in about 50% of patients with Usher type 3 [19], and the onset of RP is usually after the age of 20 years [20]. Usher type 4 represents a group of "atypical" Usher syndrome cases characterized by a late-onset moderate-to-severe sensorineural hearing loss and RP or cone-rod dystrophy with no vestibular involvement [21-24].

Here we report on a family presenting to an inherited retinal dystrophy clinic that appeared to have a form of Usher syndrome that segregated in an autosomal dominant manner. We characterized the phenotype, identified the genetic cause, and modeled the phenotype in zebrafish.

METHODS

Study participants and clinical assessment: This study was approved by the clinical research ethics board of the University of British Columbia and adhered to the tenets of the Declaration of Helsinki. A four-generation Caucasian Canadian family, originally of Scottish descent, was examined by retinal specialists in an inherited retinal dystrophy (IRD) clinic at the Eye Care Centre in Vancouver, Canada. Informed consent was obtained from all participants included in the study.

Each family member had a comprehensive ocular examination, including best-corrected visual acuity (BCVA), direct and indirect ophthalmoscopy, and slit-lamp biomicroscopy. In addition, color fundus photography (wide-field camera; Optos, Marlborough, MA), visual field testing, autofluorescence, and spectral-domain optical coherence tomography (Heidelberg Engineering, Heidelberg, Germany) were performed. Hearing was tested by standardized pure-tone audiometry (250 to 8,000 Hz) relative to hearing thresholds (normal hearing is ≤19.9 dB hearing loss [HL] in adults). The degree of HL over time was calculated using the pure-tone average (PTA) at four frequencies (0.5, 1, 2, and 4 kHz) in the better ear without amplification [25]. The degree of HL was divided into six categories, including mild (20–34.9 dB HL), moderate (35–49.9 dB HL), moderate to severe (50–64.9 dB HL), severe (65–79.9 dB HL), profound (80.0–94.9 dB HL), and complete loss (≥95 dB HL) [26].

Molecular genetic testing: Participant DNA was obtained from buccal swabs, which were screened using panel-based testing of genes associated with retinal dystrophies (Blueprint Genetics, Espoo, Finland). In silico analysis of the variant identified was evaluated with PolyPhen-2, which predicts the impact of a single amino acid substitution on the structure and function of a human protein using physical and comparative considerations; MutationTaster, which analyzes both protein and DNA, thereby assessing single amino acid variations and synonymous, intronic, and deletion variants; and SIFT, which predicts the effects of nonsynonymous single nucleotide variants and frameshifting indels on protein function. The interpretation of pathogenicity was based on criteria established by the American College of Medical Genetics and Genomics [27]. The results were correlated with the participant's clinical diagnosis, and each participant received genetic counseling regarding their test results.

Zebrafish husbandry: Research was carried out following protocols compliant with the Canadian Council on Animal Care with the approval of the Animal Care Committee at the University of British Columbia and with the Association for Research in Vision and Ophthalmology statement for the use of animals in vision research. Adult wild-type AB [28] or transgenic Tg[*TαCP:GFP*] zebrafish [29] strains were maintained at 28.5 °C on a 14-h light/12-h dark cycle in an Aquatic Habitats Aquarium (Pentair Aquatic Eco-Systems, Apopka, FL). Zebrafish were fed brine shrimp (Artemia EG; INVE Aquaculture, Salt Lake City, UT) hatched in the fish facility and flake food for tropical fish (Tetra GMBH, Melle, Germany). In the transgenic Tg[*TαCP:EGFP*] strain, the cone α-transducin promoter drives enhanced green fluorescent protein (EGFP) expression in all cone photoreceptors. After natural mating, embryos were collected and raised in E3 medium (297.7 mM NaCl, 10.7 mM KCl, 26.1 mM $CaCl_2$, and 24.1 mM $MgCl_2$) containing 1% methylene blue (Sigma-Aldrich, St. Louis, MO) at 28.5 °C.

Knockdown of tubb4b messenger RNA using morpholino oligonucleotides: A splicing-blocking *tubb4b*-MO1 (5′-AGT AAT TAG ACT CTC ACC TGT GGC T-3′), designed to prevent the messenger RNA (mRNA) splicing of *tubb4b* exon 2 to exon 3, was synthesized by GeneTools (Philomath, OR). This MO1 blocked both alternate transcripts of *tubb4b* (*tubb4b*-201 and *tubb4b*-202; Zebrafish GRCz11 genome assembly). A control mismatch morpholino oligonucleotide (MO) (*tubb4b*-MM) was also synthesized (5′-AGT AAT TAG AGT GTC ACG TGT CGC T-3′). A translation-blocking morpholino (*tubb4b*-MO2) was additionally designed (5′-CCT GTA AAT GCA CGA TCT CCC TCA T-3′) to confirm the phenotype. All *tubb4b* MOs were diluted in 1X Danieau buffer [58 mM NaCl, 0.7 mM KCl, 0.4 mM $MgSO_4$, 0.6 mM $Ca(NO_3)_2$, 5 mM hydroxyethyl piperazineethanesulfonic acid, pH 7.6] containing 0.1% phenol red. The MOs (0.75 ng) were injected into the yolk of one to two cell-stage embryos using a Nanoject II variable injector (Drummond Scientific, Broomall, PA). The morphant embryos were raised at 28.5 °C and observed for morphologic changes using a stereoscopic microscope. To aid image analysis, 0.2 mM phenylthiourea (Sigma-Aldrich, Oakville, ON, Canada) was added to the

embryos at 10 h postfertilization (hpf) to inhibit pigment formation. Embryos were fixed in 4% paraformaldehyde (PFA) at specific developmental time points, and images were captured using a Zeiss Axioplan 2 microscope with D63ZNC DVC camera (Carl Zeiss, Toronto, ON, Canada).

Western blotting: We collected 20 wild-type or morphant embryos from the *tubb4b*-MO2 knockdown at 3 days postfertilization (dpf) for western blotting by initially snap freezing them in liquid nitrogen before being homogenized by sonication in lysis buffer (10 mM Tris, pH 7.5, 10 mM NaCl, 1% sodium dodecyl sulfate, 1X Roche Protease Inhibitor Cocktail, MilliporeSigma, Oakville, ON, Canada). Insoluble material was removed by a 10-min centrifugation (25,000 × *g*). Protein concentration was determined by the DC protein assay (Bio-Rad, Mississauga, ON, Canada). Zebrafish proteins (75 µg) were separated on a 12% sodium dodecyl sulfate–polyacrylamide gel and transferred to an Immobilon-FL membrane (MilliporeSigma). The membrane was incubated in 5% nonfat milk powder in PBS/0.1% Tween-20 (PBST) for 2 h at room temperature (RT) and incubated overnight at 4 °C with primary antibody (tubb4b or gapdh). Following three washes in PBST, the membrane was incubated in the dark for 1 h with a relevant secondary antibody. After the membrane was washed three times in PBST in the dark, protein bands were visualized using a LI-COR Odyssey detector (Mandel Scientific, Guelph, ON, Canada). Commercially available antibodies used were as follows: 1:4,000 mouse monoclonal to Tubb4b (Aviva Systems Biology, San Diego, CA; cat. OAAJ03324) and 1:2,000 rabbit polyclonal to glyceraldehyde 3-phosphate dehydrogenase (GAPDH glyceraldehyde 3-phosphate dehydrogenase (GAPDH); Abcam Inc. Toronto, ON, Canada, cat. 9485). The secondary antibodies (1:5,000) used were IRDye 680RD goat anti-mouse IgG (LI-COR Biosciences, Lincoln, NE; cat. 926–68070) or IRDye 800CW goat anti-rabbit IgG (LI-COR Biosciences; cat. 926–32211).

mRNA expression studies: Total RNA was extracted from euthanized zebrafish heads using the Aurum Total RNA Mini Kit (Bio-Rad) according to the manufacturer's instructions. Using 0.5 µg total RNA, the reverse-transcription reaction was performed in a 20-µl reaction volume containing 4 mM deoxynucleotide triphosphate mix, 1X random primers, 1X RT buffer, 20 U RNase inhibitor, and 50 U RT enzyme (Applied Biosystems High Capacity cDNA Reverse Transcription Kit; ThermoFisher Scientific, Waltham, MA). The yield of complementary DNA product was evaluated by Nanodrop spectrophotometry (ThermoFisher Scientific). We used 5 ng complementary DNA as a template for amplification using the QuantiTect Reverse Transcription Kit (Qiagen, Toronto, ON, Canada). Primers for *tubb4b* (330 bp product) were forward primer 5′-CAA CAA TGA GGG AGA TCG TG-3′, reverse primer 5′-GTT CCA CGT GCC GTG CTG GT-3′; primers for *rhodopsin* (405 bp product) were forward primer 5′-AGT CCT GCC CAG ACA TCT AG-3′, reverse primer 5′-CGA CCA TAG CCC CAT CTC AC-3′; primers for *tubb6* (268 bp product) were forward 5′-AGT GTT CGT TCT GGA GCG TT-3′, reverse 5′-ATG ATG CGG TCC GGG TAT TC-3′; and primers for *gapdh* (190 bp product) were forward primer 5′-CAC CAG GGC TGC TTT TAA C-3′, reverse primer 5′-ATC TCG CTC CTG GAA GAT C-3′. Thermocycling parameters were as follows: 2 min at 50 °C, 20 s at 95 °C, 40 cycles of 1 s at 95 °C, plus 20 s at 58 °C. ImageJ software (National Institutes of Health, Bethesda, MD) was used to quantify band intensities relative to gapdh.

RESULTS

Ocular phenotype: Four affected members and four unaffected members of a four-generation Canadian family were examined at an IRD specialist clinic with a phenotype of hearing loss and RP. This deaf-blind syndrome segregated in an autosomal dominant manner (Figure 1). Clinical data for this family are presented in Table 1. The male proband (III-4) presented in 2012 at 50 years of age, reporting poor vision since age 23. He also reported hearing loss from 9 years of age. His BCVA at age 50 had been 20/20 right and 20/30 left. Anterior segment examination was unremarkable. Dilated fundus examination revealed mid-peripheral chorioretinal atrophy with bone spicule retinal degeneration extending into the far periphery (Figure 2). Goldmann visual field testing from 2009 showed extensive mid-peripheral field loss with preservation of the central 10 degrees in each eye and some far peripheral field retention (Figure 3). Further testing at 55 years old and 62 years old revealed progression of bone spicule retinal degeneration (Figure 2) and further loss of far peripheral visual field (Figure 3).

The proband's older brother (III-1) presented at 60 years of age. He reported night blindness from the age of 17 years and deafness from early childhood. His visual acuity at age 60 was 20/40 right and 20/50 left. A dilated fundus examination showed optic nerve pallor in both eyes with extensive mid-peripheral chorioretinal atrophy (Figure 4). Visual field testing at 61 years of age showed near-mid-peripheral loss confined between 5 and 30 degrees, consistent with a diagnosis of pericentral retinitis pigmentosa (Figure 3). Field loss was less severe than in his younger brother.

The proband's younger sister (III-6) presented in 2023 at 54 years of age and reported vision loss from 32 years of age and hearing loss from 37 years old. BCVA was 20/70 right and finger counting only left. Retinal imaging showing

Table 1. Patient clinical phenotype summary.

Family ID	Age*	Sex	Retinal phenotype	Hearing loss (HL)
III-1	60	M	Night-blindness at 17 years. BCVA: R 20/40, L 20/50. Optic nerve pallor, near mid-peripheral chorioretinal atrophy.	Began at 10 years. PTA 67.5 dB HL, MS-S.
III-3	57	M	No symptoms. BCVA: R/L 20/20. Normal retina examination.	No HL
III-4 proband	50	M	Night-blindness at 23 years. BCVA: R 20/20, L 20/30. Bone spicule retinopathy extending into the far periphery in each eye.	Began at 9 years. PTA 57.5 dB HL, M-MS.
III-6	58	F	Poor vision at 32 years. BCVA: R 20/70, L, finger counting only. Mid peripheral chorioretinal atrophy with macular sparing.	Began at 37 years. PTA 45.0 dB HL, M-MO.
IV-1	20	F	No symptoms. BCVA: R/L 20/25; normal retina exam.	No HL
IV-2	31	F	No symptoms. BCVA: R/L 20/20; normal retina exam; no VF defect.	No HL
IV-3	29	F	No symptoms. BCVA: R/L 20/20; normal fundus exam; no VF defect.	No HL
IV-4	24	M	No symptoms. BCVA: R/L 20/20; Mild pigmentary retinopathy.	Began at 16 years. PTA 43.7 dB HL, MO.

*, Age at presentation; M, male; F, female; BCVA, best corrected visual acuity; VF, visual field; PTA4, most recent pure tone average threshold for frequencies of 0.5, 1, 2 and 4 kHz; M-MO, mild-to-moderate; M-MS, mild-to moderately severe; MO, moderate; MS-S, moderately-severe to severe.

extensive chorioretinal atrophy with visual fields restricted to just 2 degrees or less.

The proband's son (IV-4) presented in 2021 at 24 years of age with no visual symptoms but recent mild hearing loss. BCVA was 20/20 right and left. Clinical examination revealed minor bone spicule pigmentary changes in the left eye and retinal pigment epithelial anomalies in the mid-periphery of both eyes. Goldmann visual fields were normal.

Hearing phenotype: Both first and second generations of the family were reported by the proband as being deaf and blind but were not examined in the clinic. The proband reported poor hearing since he was 11 years old, and this was not corrected during his school years. He started using hearing aids at age 22. An auditory test at age 28 showed bilateral mild-to-moderate mid-frequency sensorineural hearing loss with a PTA (at 0.5, 1, 2, and 4 K frequencies) of 42.5 dB HL (Figure 5A). The progression to moderately severe was

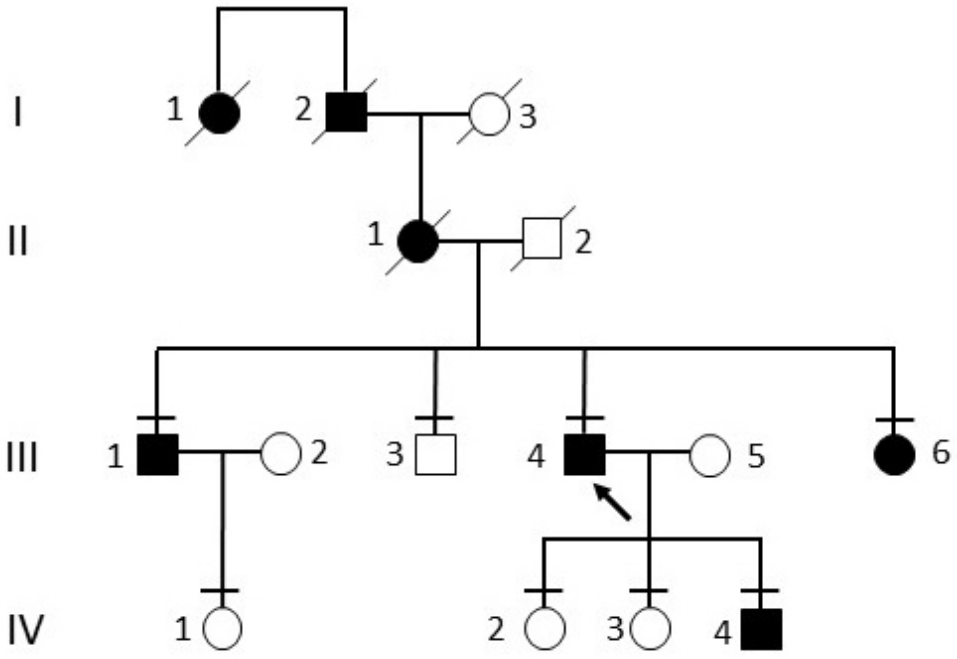

Figure 1. Four-generation family tree segregating autosomal dominant hearing loss and RP. The black symbols represent affected individuals and white symbols represent unaffected individuals. The arrow indicates the proband patient. The line above the symbols denotes family members who were examined. The first two generations were reported by proband as deaf-blind but were not examined or genetically tested.

recorded at age 40 (PTA 56.6 dB HL). In the most recent audiometry test at age 60, he had mild-to-moderately severe hearing loss with a PTA of 57.5 dB HL (Figure 5A). His son (IV-4) at age 9 had a normal audiometry test, but at age 16, he was found to have a mild bilateral sensorineural hearing loss in the 1,000 to 4,000 Hz range (PTA 26.25 dB HL; Figure 5B). At age 22, this had progressed to moderate hearing loss (PTA 43.7 dB HL; Figure 5B), and thus he started wearing

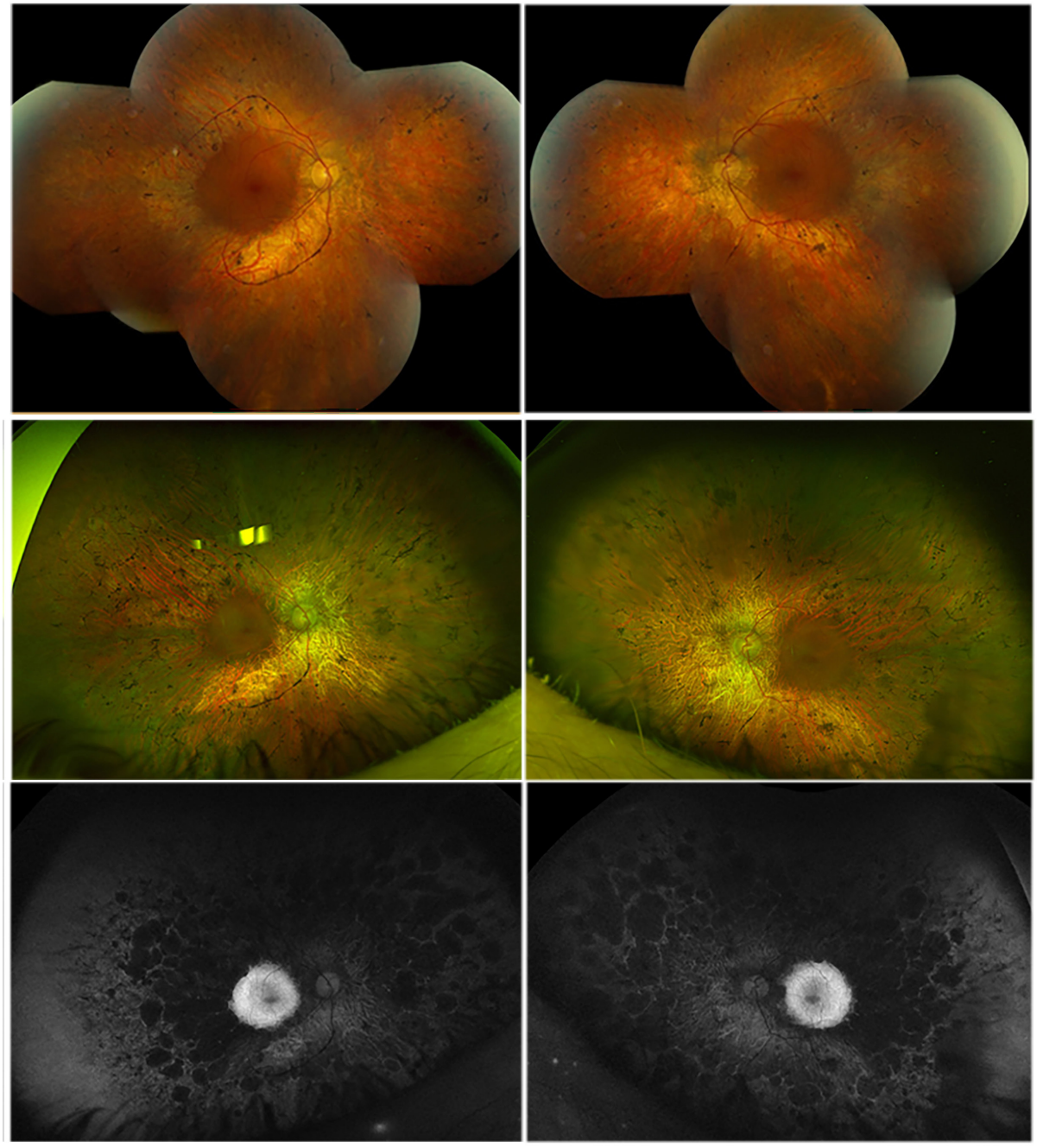

Figure 2. Color fundus and autofluorescence images from affected participant III-4. The upper row are color fundus images from age 51 years showing bone spicule retinal degeneration extending into the peripheral retina. The middle row shows color fundus images from age 62 years showing further extension of bone spicule retinal degeneration into the macular area and peripheral retina. Bottom row, autofluorescence imaging showing widespread hypo-autofluorescence plus hyper-autofluorescence at each macula. This would be described as typical retinitis pigmentosa.

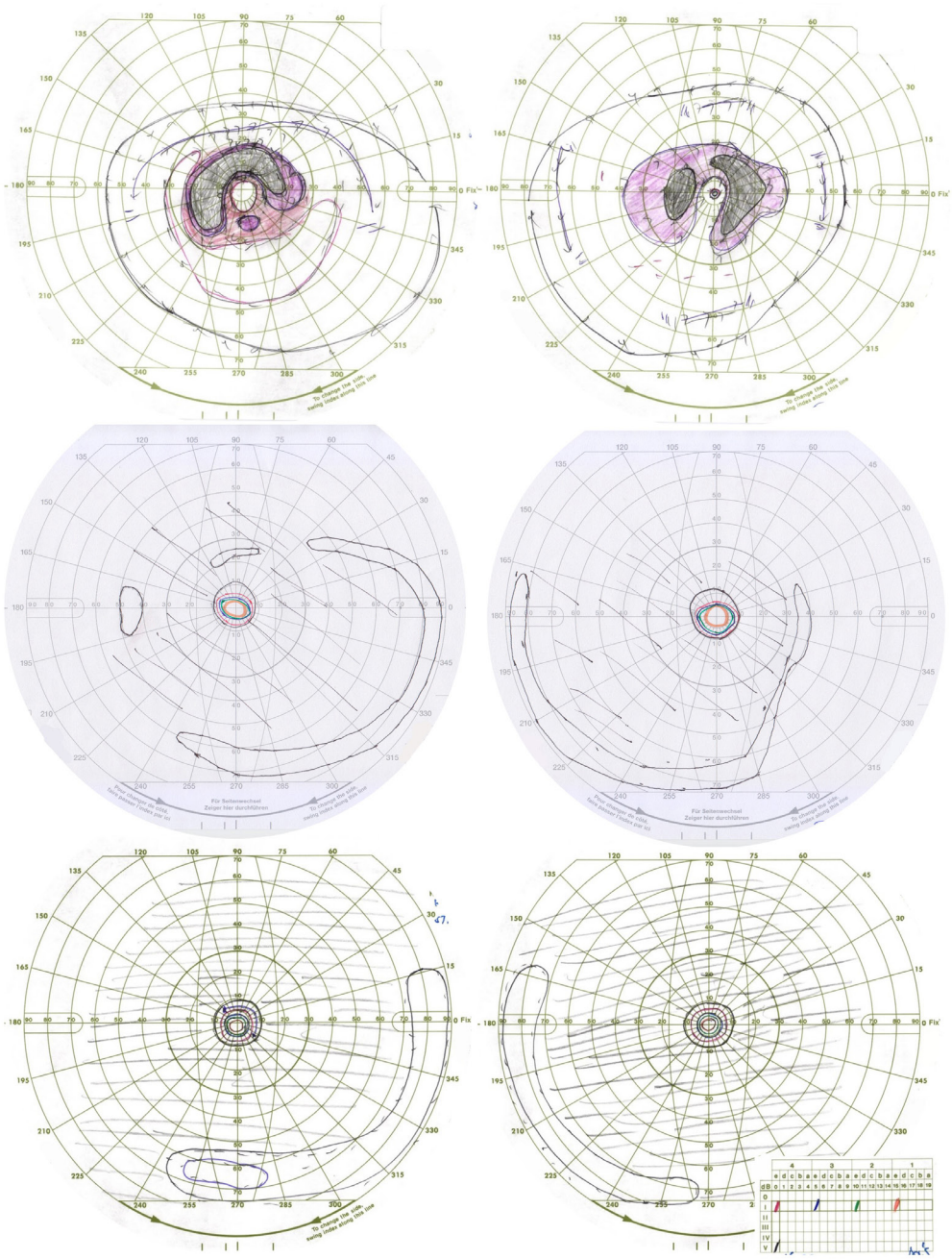

Figure 3. Deidentified Goldmann visual field results from affected participants III-1 and III-4. The upper row shows results from participant III-1 at 61 years of age showing dense mid-peripheral ring scotomas extending from 5 to 30 degrees. The middle row shows results from participant III-4 at 43 years old showing extensive field loss beyond the mid-periphery. The bottom row shows results from participant III-4 at 55 years of age showing further decline of far peripheral islands of vision.

hearing aids. The elder brother of the proband (III-1) had hearing loss since childhood, and his most recent audiometry test at age 57 showed he had bilateral moderately severe to severe sensorineural hearing loss with a PTA of 67.5 dB HL (Figure 5C). The sister of the proband (III-6) noticed hearing loss in the third decade of life. Her most recent audiometry test was at age 51, when she exhibited bilateral mild-to-moderate sensorineural hearing loss, with a PTA of 45.0 dB HL (Figure 5D). She started wearing hearing aids at age 51.

Family members III-3, IV-1, IV-2, and IV-3 did not report any hearing loss.

Genetic testing results: Since the clinical phenotype resembled that of Usher syndrome, we expected to see variants in the known Usher syndrome genes. However, upon panel-based genetic testing in 2019 (266 genes), the proband had three variants of uncertain significance: *ADAMTS18* [c.570C>G, p.(Asn190Lys)], *USH2A* [c.12611C>T, p.(Thr4204Met)], and *WFS1* [c.2494C>T, P.(Arg832Cys)]. *ADAMTS18* and USH2A are inherited in a recessive manner, so they are unlikely to explain the phenotype in the patient. In addition, in the Leidon Open Variation Database for USH2A, the p.(Thr4204Met) USH2A variant is reported as benign. *WFS1* variants cause Wolfram syndrome (optic atrophy, sensorineural hearing loss, and dysarthria) and can be inherited in recessive and dominant forms. However, the specific *WFS1* variant we found is relatively common in the gnomAD reference database, and the patient did not have optic atrophy, so it seems unlikely to be the cause of the phenotype. Another member of the family (III-1) was tested in 2021 when the gene panel was larger (285 genes), and a single missense variant in the *TUBB4B* gene (c.1168C>T, p.(Arg390Trp) was identified, which was previously reported as a mutation hotspot [30]. In silico modeling for this variant with Polyphen-2 predicted it was probably

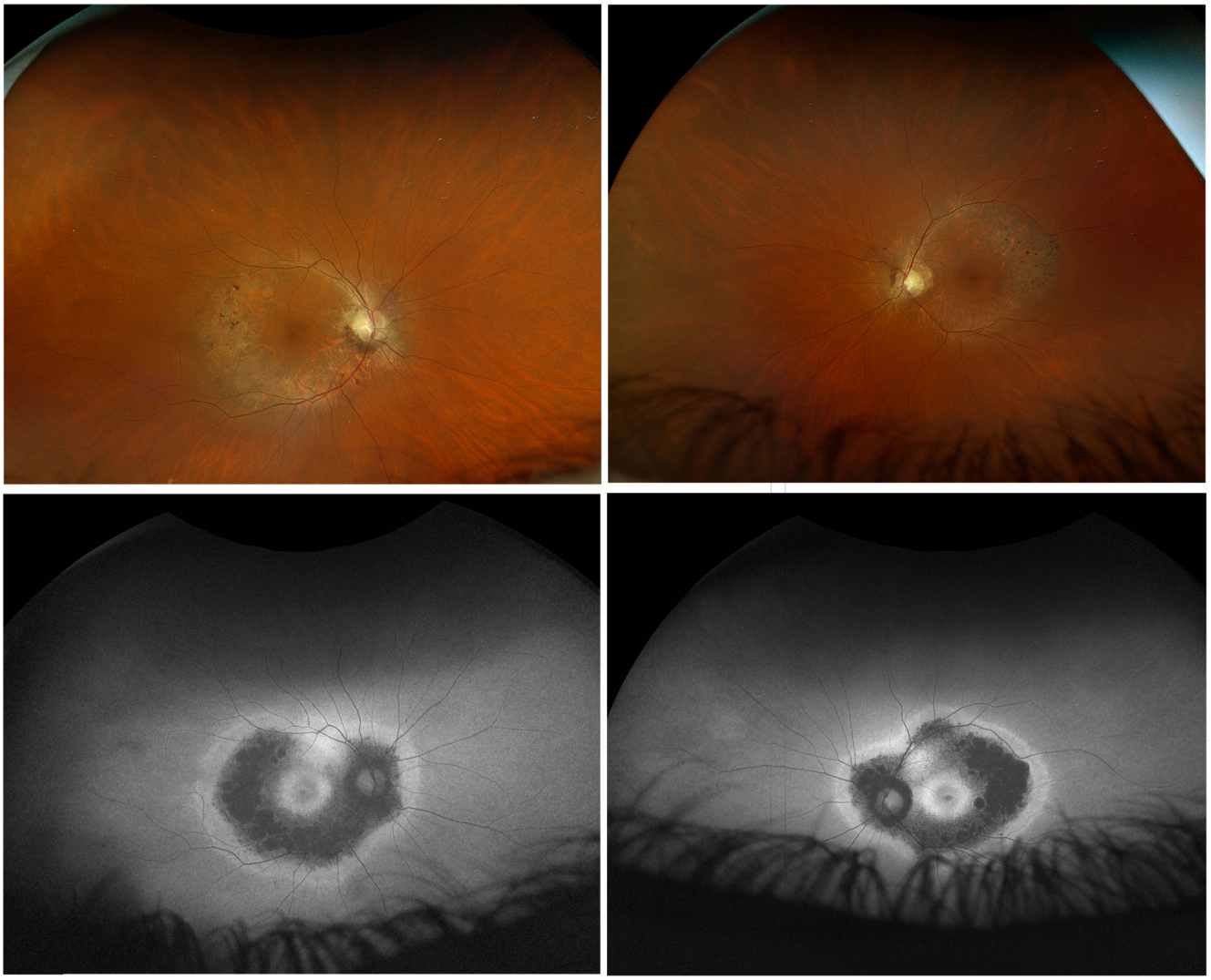

Figure 4. Color fundus and autofluorescence images from affected participant III-1. The upper row shows color fundus images from age 63 years showing bone spicule retinal degeneration confined to the near periphery. The bottom row shows autofluorescence imaging showing a hypo-autofluorescence band confined to the posterior pole plus hyper-autofluorescence beyond this area and at each macula. This would be described as pericentral retinitis pigmentosa.

damaging; with SIFT modeling, it was predicted to be deleterious; with MutationTaster modeling, the prediction was disease-causing. Missense variants in *TUBB4B* (Table 2) had been recently reported in association with dominantly inherited Leber congenital amaurosis with early-onset deafness [31]. We therefore tested the rest of the family and retested the proband (as *TUBB4B* was not on the genetic testing panel at first testing). Indeed, we found all affected family members had the same *TUBB4B* variant, and none of the unaffected members carried the variant. Importantly, family member IV-4 did not have the *WFS1* variant that his father had, ruling out *WFS1* as a cause of the dominant disease in the family.

Loss-of-function testing: We used morpholino gene knockdown technology to provide functional evidence that *tubb4b* is important to ocular development [32]. Injection of a mismatch control morpholino did not affect wild-type at 72 hpf, but injection of either splice-blocking or translation-blocking *tubb4b* morpholinos resulted in morphants displaying cardiac edema and hydrocephalus (Figure 6). Immunohistological analysis of the retina revealed a loss of cone photoreceptors, as demonstrated by a reduction in cone green fluorescent protein (GFP) expression in the *TαCP:EGFP* transgenic retina for both morpholinos. Confirmation of the effectiveness of splice-blocking MO1 was determined by reverse transcription (RT)-PCR since this would result in loss of *tubb4b* exon

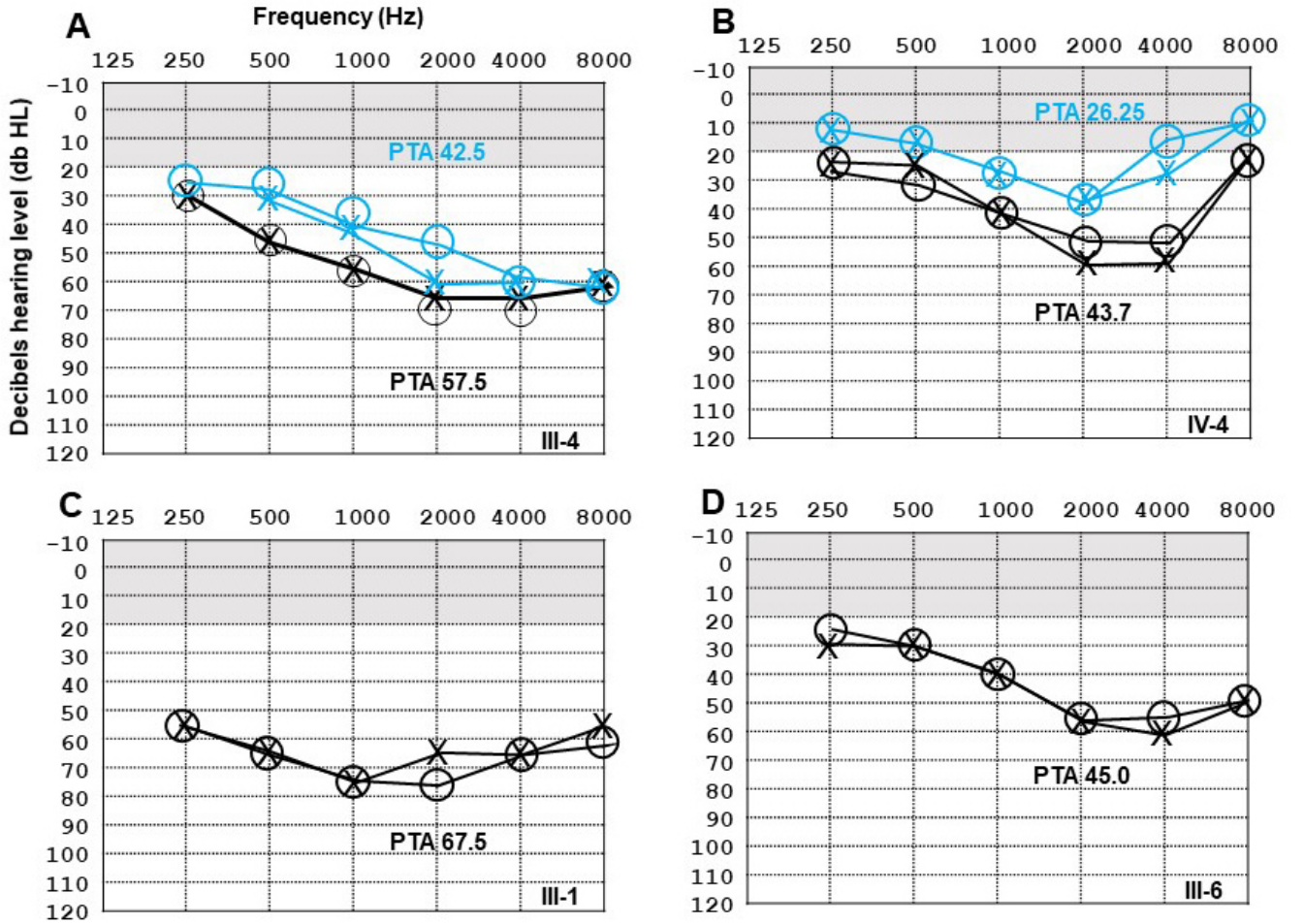

Figure 5. Audiograms for affected members of the family. Normal hearing range is highlighted by gray boxes (≤19.9 db HL) and specific family members denoted in the bottom right corner of the plot. (**A**) Hearing test in proband III-4. The X symbol is data from the left ear and the circle symbol is data from the right ear. Blue traces at age 28 and black traces at age 60 show progression of hearing loss over time. PTA scores are denoted in a corresponding color. (**B**) Hearing test in son of proband (IV-4). Blue traces at age 16 and black traces at age 22 show progression of hearing loss over time. (**C**) Hearing test in brother of proband (III-1). Audiogram traces at age 57 show severe hearing loss (PTA highest of all members tested). (**D**) Hearing test in sister of proband (III-6). Audiogram traces at age 51 correspond to lower hearing loss (PTA 45.0) compared to her two siblings (**A** and **C**).

2 in the mRNA transcript (Figure 7A,B). Confirmation of the effectiveness of translation-blocking morpholino MO2 was determined by tubb4b western blotting, where tubb4b protein was not detected (Figure 7C). To test for loss of rod photoreceptors in embryos injected with translation-blocking MO2, we used semiquantitative RT-PCR to examine the relative number of rhodopsin transcripts and found an 82% ± 7% (standard error of the mean, n = 3) reduction, reflecting a lower number of rods present in the retina (Figure 7D). In a recently reported mouse *Tubb4b* knockdown experiment, *Tubb6b* was upregulated as a compensatory mechanism for the loss of *Tubb4b* [33]. Using semiquantitative RT-PCR normalizing gene expression to GAPDH, we found that expression of *tubb6* was unchanged in the *tubb4b* morphants (Figure 7D).

DISCUSSION

In our study, we identified a four-generation family segregating a p.(Arg390Trp) *TUBB4B* variant with RP and late-onset, progressive sensorineural hearing loss inherited in an autosomal dominant manner. To our knowledge, this is the first reported family with this phenotype. There is recent literature supporting *TUBB4B* variants in association with retinopathy segregating with hearing loss at two mutation

Table 2. *TUBB4B* variants and associated phenotypes.

Reported *TUBB4B* variants	Hearing loss (HL) onset (yr), respectively	Eye disease onset (yr), respectively	Phenotype	References
c.1168C>T, p.(Arg390Trp)				
Canadian family - 4 affected patients	10, 11, 37, 16 year	17, 23, 32, 27 year	RP, nyctalopia, VF loss	**This paper**
German simplex case	NR, severe HL at 36 year	36 year	Reduced ERG, ring atrophy	Bodenbender et al., 2024
c.1172G>A, p.(Arg391His)				
3 French /1 Algerian family	birth, 3, 7, 8 year	birth x 2, 2.5, 3 year	LCAEOD	Luscan et al., 2017
1 American de novo case	3 year	6 year	LCAEOD, VD	Medina et al., 2021
1 German mosaic (24%) case	17yr	17yr	Nyctalopia, atrophic areas, reduced ERG	Bodenbender et al., 2024
c.1171C>T, p.(Arg391Cys)				
Danish de novo case	birth	birth	LCAEOD	Luscan et al., 2017
1 Chinese de novo case	8 months	2 year	LCAEOD, VD	Medina et al., 2021
Hungarian family - 3 affected patients	NR in 2 patients, 3.5 year	7 months, 2.75 year, 3 year	LCAEOD	Maasz et al. 2022
German simplex case	NR, moderate HL at 24 year	4yr	Atrophic lesions, reduced ERG	Bodenbender et al., 2024
c.1169G>A, p.(Arg390Gln)				
German family - 2 affected patients	NR, moderate HL at 69 year, no HL at 39 year	30 and 25 year	Ring atrophy, BS, Reduced ERG	Bodenbender et al., 2024
c.928T>C, p.(Tyr310His)				
German de novo case (VUS)	birth	1 year	Reduced ERG	Bodenbender et al., 2024
c.32A>G, p.(Gln11Arg)				
American de novo case	birth	6 months	Hyperopia, micro-cornea, plus FS	McFadden et al., 2023
c.1072C>T, p.(Pro358Ser)				
4 de novo cases 3 Caucasian / 1 African	1.5, 14, 11, 10 year	1.5, 14, 11, 10 year	LCAEOD plus primary ciliary dyskinesia	Dodd et al., 2024

yr, years; mo, months; NR, not recorded; ERG, electroretinogram; LCAEOD, Leber congenital amaurosis and early-onset deafness; RP, retinitis pigmentosa; BS, bone spicules; VF, visual field; VD, vestibular dysfunction; FS, Faconi syndrome.

hotspots [30]. Two ultra-rare variants in the *TUBB4B* gene were initially reported to segregate with Leber congenital amaurosis with early-onset deafness: p.(Arg391His) and p.(Arg391Cys) [31,34]. A de novo variant p.(Gln11Arg) was also identified in an American female child with hearing loss, Faconi syndrome, rickets, and microphthalmia but without retinal abnormalities [35]. Four unrelated de novo cases had a p.(Pro358Ser) *TUBB4B* variant that was associated with Leber congenital amaurosis, sensorineural hearing loss, and primary ciliary dyskinesia [36].

Also recently, Bodenbender and colleagues described three variants [30]: a p.(Arg390Gln) variant segregated in a mother and son with late-onset night blindness and symptomless-to-moderate hearing loss; a de novo p.(Tyr310His) variant was found in a female infant with congenital profound hearing loss and reduced electroretinographic responses but without a specific retinal diagnosis. Most importantly, Bodenbender and colleagues reported a p.(Arg390Trp) variant in a single 36-year-old patient who reported glare sensitivity only and hearing loss. On further analysis, he was found to have a reduced electroretinographic response and thinning of the outer retina on optical coherence tomography imaging. Segregation of this variant was not available.

To our knowledge, the study is the first to report the *TUBB4B* variant p.(Arg390Trp) segregating with disease in an extended pedigree, establishing autosomal dominant inheritance. A comparison of retinal phenotypes also distinguishes the *TUBB4B* variant p.(Arg390Trp) phenotype seen in our study in comparison to the *TUBB4B* variant p.(Arg390Trp) phenotype reported by Bodenbender and colleagues [30]. In that simplex case, the retinal phenotype was described as a pericentral RP, whereas proband III-4 in our study is clearly better described as having a more extensive, typical RP (Figure 2 and Figure 3). Participant III-1 could be described as having a case of pericentral RP, which is described as milder and more slowly progressive than typical RP (Figure 3 and Figure 4). We conclude that unlike the report in Bodenbender and colleagues [30], we cannot confirm a solely mild retinal phenotype to the *TUBB4B* variant p.(Arg390Trp) but more accurately portray it as variable, with pericentral or typical retinitis pigmentosa subtypes possible.

It can also be concluded from the literature to date that six *TUBB4B* variants targeting four codons are associated with deaf-blindness. Variants at either codon Arg390 or Arg391 are restricted to phenotypes with hearing loss and retinal disease, whereas codons Gly11 and Pro358 are

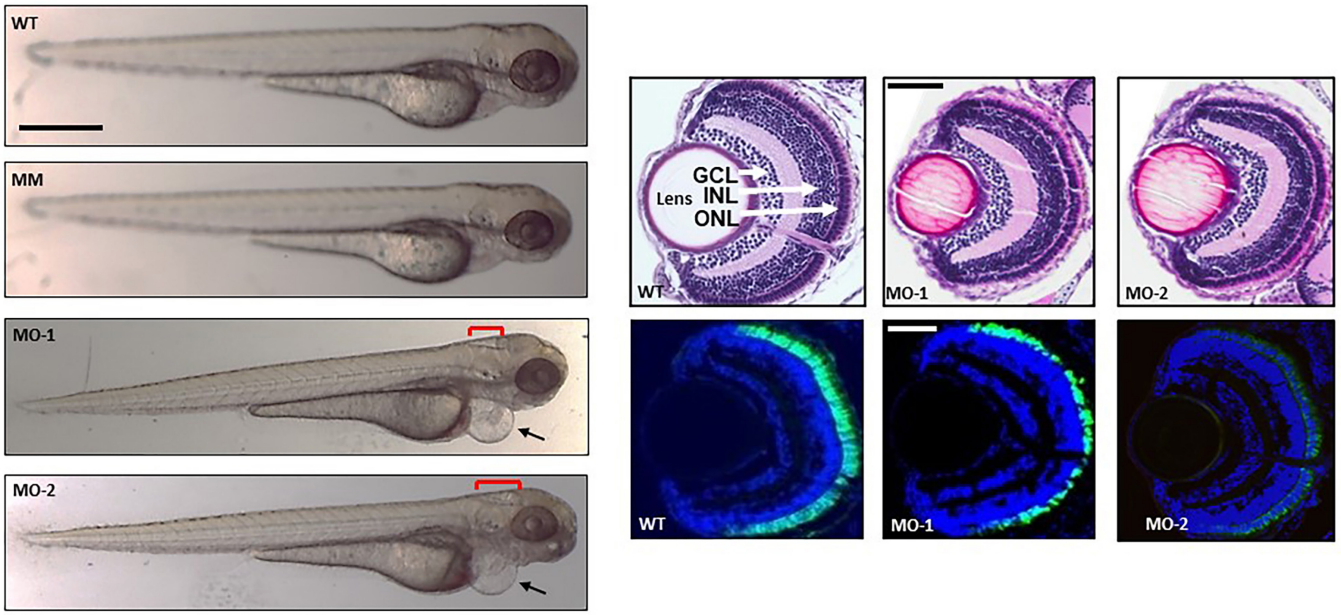

Figure 6. *tubb4b* loss-of-function phenotype in zebrafish observed at 72 hpf. The left panels show whole larvae morphology. MO-1 refers to *tubb4b*-specifc splice-blocking morpholino; MO-2, *tubb4b*-specifc translation-blocking morpholino; MM, mismatch control morpholino; WT refers to wild-type phenotype zebrafish. The arrow identifies cardiac edema and the red brackets shows hydrocephalus [204 ± 10 µm (standard error of the mean, n = 15) in MO-1 and 272 ± 12 µm (standard error of the mean, n = 12) in MO-2]. The size bar equals to 500 µm. The top row of the right panels show histologic sagittal sections through the retina and the bottom rows compare expression of EGFP (green) in cone photoreceptor cells in *TαCP:EGFP* transgenic fish with MO-1 or MO-2 treatment. GCL-ganglion cell layer; INL-inner nuclear layer; ONL-outer nuclear layer. The size bar equals 500 µm.

associated with deaf-blindness and a broader range of systemic ciliopathies.

To understand how variants in *TUBB4B* cause retinal and hearing loss phenotypes, we knocked down the *tubb4b* gene in zebrafish and found loss of both rod and cone photoreceptors, as well as hydrocephalus, which caused lethality by 5 dpf. In the developing otic vesicle, we did not observe structural abnormalities in the otoliths (ear stones) at 72 hpf, which are connected to the kinocilia of hair cells and are necessary for detecting sound and sensing linear accelerations in zebrafish [37]. However, the developing inner ear does not reach full maturity until 20 dpf [38], and thus we cannot be certain that there are no hearing defects in the *tubb4b* morphant larvae. Since the knockdown is lethal, we were not able to take advantage of detecting auditory defects at 5 dpf by analyzing startle reflex responses [39]. Future studies creating zebrafish *tubb4b* knock-in mutants may allow long-term studies to resolve whether the mutants have hearing loss and for testing possible therapeutic approaches.

In two recent studies, targeted deletion of the *Tubb4b* gene in mice resulted in hydrocephaly and perinatal lethality [36,40] similar to our zebrafish data. Generation of a mouse line carrying a mutation equivalent to a known human mutation (*Tubb4b*$^{R391H/+}$) resulted in mice that were infertile due to a spermatogenesis defect, but they did not develop any retinal degeneration [37]. The mice had profound deafness due to motility defects in epithelial cells of the middle ear and decreased microtubules in pillar support cells in the inner ear. It was further demonstrated that a compensatory upregulation of *Tubb6* mRNA and protein in the knockout mice could be why there was an absence of a retinal phenotype in mouse mutants [33]. We also tested *tubb6* expression in the zebrafish morphants and did not find any upregulation of *tubb6* mRNA, suggesting there is no compensatory mechanism in zebrafish. Thus, although the *Tubb4b* mouse models are excellent for

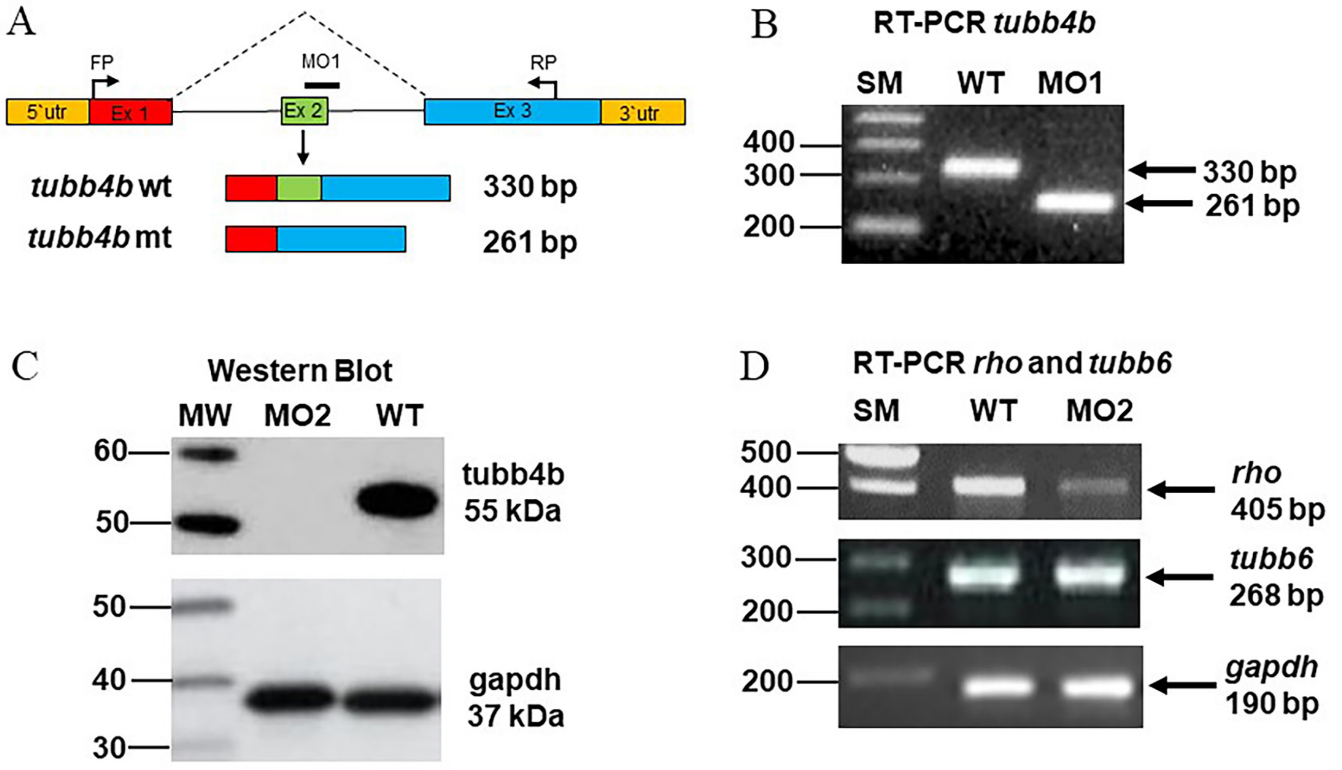

Figure 7. This figure shows confirmation of *tubb4b* morpholino knockdown. (**A**) Schematic representation of MO-1 splice-blocking that removes exon 2 (Ex 2) in the mutant (mt) mRNA transcript. FP refers to the forward primer; RP refers to the reverse primer; utr refers to the untranslated region. (**B**) Representative RT-PCR gel confirming reduction in size of *tubb4b* amplicon. MO1 refers to splice-blocking morpholino; SM refers to size marker; WT refers to the wild-type. (**C**) Representative image of a western blot of tubb4b protein in zebrafish injected with MO2 translation-blocking morpholino. The gel loading control is gapdh. MW refers to molecular weight size marker and WT refers to the wild-type. (**D**) Representative RT-PCR gels showing levels of rhodopsin (*rho*) and *tubb6* transcripts with MO2 translation-blocking morpholino knockdown relative to *gapdh* expression.

studying hearing loss, they are not useful for studying vision loss. One possibility may be to generate a *Tubb4b* mutant on a *Tubb6* knockout background to elicit an eye phenotype. A similar disconnect in phenotype is seen with mouse models of Usher syndrome type 1B due to abnormalities in the *Myo7a* gene, in which hearing loss is present with only subtle retinal phenotypes [41]. This has been explained by a difference in the structure of mouse and human photoreceptors, where calyceal processes expressing MYO7A are absent in mice [42]. Further studies in human tissue analyzing expression of TUBB4B in calyceal processes may explain the lack of phenotype in mice.

Conclusions: In summary, we have identified a *TUBB4B* disease-causing variant in a four-generation family segregating deafness and RP, which expands the clinical phenotype associated with *TUBB4B* gene variants. To our knowledge, this is the first time a *TUBB4B* variant has been reported as segregating with disease in an extended family, establishing autosomal dominant inheritance. We also expand the range of phenotype seen with the typical RP phenotype in addition to the pericentral phenotype previously documented. This phenotype could represent a dominant form of Usher syndrome type 3, characterized by postlingual sensorineural hearing loss and RP without vestibular involvement. Due to the high level of gene conservation, loss of function of *Tubb4b*/*tubb4b* leads to early lethality in both mice and zebrafish and suggests that homozygous variants in *TUBB4B* in humans might also be embryonic lethal. Since the *tubb4b* zebrafish model demonstrates an eye phenotype unlike mice, this could become the best model to test potential therapeutic options for the retinal phenotype.

ACKNOWLEDGMENTS

This work was supported by the Fighting Blindness Canada Patient Registry (grant number F22-04266_20240521). Declaration of interest statement. The authors state they have no conflicts of interest to declare.

REFERENCES

1. Dammeyer J. Prevalence and aetiology of congenitally deafblind people in Denmark. Int J Audiol 2010; 49:76-82. [PMID: 20151880].

2. Yazigi A, De Pecoulas AE, Vauloup-Fellous C, Grangeot-Keros L, Ayoubi J-M, Picone O. Fetal and neonatal abnormalities due to congenital rubella syndrome: a review of literature. J Matern Fetal Neonatal Med 2017; 30:274-8. [PMID: 27002428].

3. Oldenski R. Cogan syndrome: autoimmune-mediated audiovestibular symptoms and ocular inflammation. J Am Board Fam Pract 1993; 6:577-81. [PMID: 8285096].

4. Mathur P, Yang J. Usher syndrome: Hearing loss, retinal degeneration and associated abnormalities. Biochim Biophys Acta 2015; 1852:406-20. [PMID: 25481835].

5. Forsythe E, Beales PL. Bardet-Biedl syndrome. Eur J Hum Genet 2013; 21:8-13. [PMID: 22713813].

6. Hsu P, Ma A, Wilson M, Williams G, Curotta J, Munns CF, Mehr S. CHARGE syndrome: a review. J Paediatr Child Health 2014; 50:504-11. [PMID: 24548020].

7. Waardenburg PJ. A new syndrome combining developmental anomalies of the eyelids, eyebrows and nose root with pigmentary defects of the iris and head hair and with congenital deafness. Am J Hum Genet 1951; 3:195-253. [PMID: 14902764].

8. Boothe M, Morris R, Robin N. Stickler syndrome: a review of clinical manifestations and the genetics evaluation. J Pers Med 2020; 10:105-[PMID: 32867104].

9. Marshall JD, Hinman EG, Collin GB, Beck S, Cerqueira R, Maffei P, Milan G, Zhang W, Wilson DI, Hearn T, Tavares P, Vettor R, Veronese C, Martin M, So WV, Nishina PM, Naggert JK. Spectrum of ALMS1 variants and evaluation of genotype-phenotype correlations in Alström syndrome. Hum Mutat 2007; 28:1114-23. [PMID: 17594715].

10. Boughman JA, Vernon M, Shaver KA. Usher syndrome: definition and estimate of prevalence from two high-risk populations. J Chronic Dis 1983; 36:595-603. [PMID: 6885960].

11. Yan D, Liu XZ. Genetics and pathological mechanisms of Usher syndrome. J Hum Genet 2010; 55:327-35. [PMID: 20379205].

12. Kimberling WJ, Hildebrand MS, Shearer AE, Jensen ML, Halder JA, Trzupek K, Cohn ES, Weleber RG, Stone EM, Smith RJ. Frequency of Usher syndrome in two pediatric populations: Implications for genetic screening of deaf and hard of hearing children. Genet Med 2010; 12:512-6. [PMID: 20613545].

13. Delmaghani S, El-Amraoui A. The genetic and phenotypic landscapes of Usher syndrome: from disease mechanisms to a new classification. Hum Genet 2022; 141:709-35. [PMID: 35353227].

14. Ebermann I, Phillips JB, Liebau MC, Koenekoop RK, Schermer B, Lopez I, Schäfer E, Roux AF, Dafinger C, Bernd A, Zrenner E, Claustres M, Blanco B, Nürnberg G, Nürnberg P, Ruland R, Westerfield M, Benzing T, Bolz HJ. PDZD7 is a modifier of retinal disease and a contributor to digenic Usher syndrome. J Clin Invest 2010; 120:1812-23. [PMID: 20440071].

15. Jacobson SG, Cideciyan AV, Gibbs D, Sumaroka A, Roman AJ, Aleman TS, Schwartz SB, Olivares MB, Russell RC, Steinberg JD, Kenna MA, Kimberling WJ, Rehm HL, Williams DS. Retinal disease course in Usher syndrome 1B due to MYO7A mutations. Invest Ophthalmol Vis Sci 2011; 52:7924-36. [PMID: 21873662].

16. Van Aarem A, Wagenaar M, Pinckers AJ, Huygen PL, Bleeker-Wagemakers EM, Kimberling BJ, Cremers CW. Ophthalmologic findings in Usher syndrome type 2A. Ophthalmic Genet 1995; 16:151-8. [PMID: 8749051].

17. Ness SL, Ben-Yosef T, Bar-Lev A, Madeo AC, Brewer CC, Avraham KB, Kornreich R, Desnick RJ, Willner JP, Friedman TB, Griffith AJ. Genetic homogeneity and phenotypic variability among Ashkenazi Jews with Usher syndrome type III. J Med Genet 2003; 40:767-72. [PMID: 14569126].

18. Adato A, Vreugde S, Joensuu T, Avidan N, Hamalainen R, Belenkiy O, Olender T, Bonne-Tamir B, Ben-Asher E, Espinos C, Millán JM, Lehesjoki AE, Flannery JG, Avraham KB, Pietrokovski S, Sankila EM, Beckmann JS, Lancet D. USH3A transcripts encode clarin-1, a four-transmembrane-domain protein with a possible role in sensory synapses. Eur J Hum Genet 2002; 10:339-50. [PMID: 12080385].

19. Millán JM, Aller E, Jaijo T, Blanco-Kelly F, Gimenez-Pardo A, Ayuso C. An update on the genetics of usher syndrome. J Ophthalmol 2011; 2011:417217[PMID: 21234346].

20. Herrera W, Aleman TS, Cideciyan AV, Roman AJ, Banin E, Ben-Yosef T, Gardner LM, Sumaroka A, Windsor EA, Schwartz SB, Stone EM, Liu XZ, Kimberling WJ, Jacobson SG. Retinal disease in Usher syndrome III caused by mutations in the clarin-1 gene. Invest Ophthalmol Vis Sci 2008; 49:2651-60. [PMID: 18281613].

21. Khateb S, Kowalewski B, Bedoni N, Damme M, Pollack N, Saada A, Obolensky A, Ben-Yosef T, Gross M, Dierks T, Banin E, Rivolta C, Sharon D. A homozygous founder missense variant in arylsulfatase G abolishes its enzymatic activity causing atypical Usher syndrome in humans. Genet Med 2018; 20:1004-12. [PMID: 29300381].

22. Ullah F, Zeeshan Ali M, Ahmad S, Muzammal M, Khan S, Khan J, Ahmad Khan M. Current updates on genetic spectrum of usher syndrome. Nucleosides Nucleotides Nucleic Acids 2024; 8:1-24. [PMID: 38718411].

23. Fu Q, Xu M, Chen X, Sheng X, Yuan Z, Liu Y, Li H, Sun Z, Li H, Yang L, Wang K, Zhang F, Li Y, Zhao C, Sui R, Chen R. *CEP78* is mutated in a distinct type of Usher syndrome. J Med Genet 2017; 54:190-5. [PMID: 27627988].

24. Fuster-García C, García-García G, Jaijo T, Fornés N, Ayuso C, Fernández-Burriel M, Sánchez-De la Morena A, Aller E, Millán JM. High-throughput sequencing for the molecular diagnosis of Usher syndrome reveals 42 novel mutations and consolidates CEP250 as Usher-like disease causative. Sci Rep 2018; 8:17113-[PMID: 30459346].

25. Sadeghi AM, Cohn ES, Kimberling WJ, Halvarsson G, Möller C. Expressivity of hearing loss in cases with Usher syndrome type IIA. Int J Audiol 2013; 52:832-7. [PMID: 24160897].

26. Olusanya BO, Davis AC, Hoffman HJ. Hearing loss grades and the *International classification of functioning, disability and health.* Bull World Health Organ 2019; 97:725-8. [PMID: 31656340].

27. Richards S, Aziz N, Bale S, Bick D, Das S, Gastier-Foster J, Grody WW, Hegde M, Lyon E, Spector E, Voelkerding K, Rehm HL. ACMG Laboratory Quality Assurance Committee. Standards and guidelines for the interpretation of sequence variants: a joint consensus recommendation of the American College of Medical Genetics and Genomics and the Association for Molecular Pathology. Genet Med 2015; 17:405-24. [PMID: 25741868].

28. Johnson SL, Midson CN, Ballinger EW, Postlethwait JH. Identification of RAPD primers that reveal extensive polymorphisms between laboratory strains of zebrafish. Genomics 1994; 19:152-6. [PMID: 8188217].

29. Kennedy BN, Alvarez Y, Brockerhoff SE, Stearns GW, Sapetto-Rebow B, Taylor MR, Hurley JB. Identification of a zebrafish cone photoreceptor-specific promoter and genetic rescue of achromatopsia in the *nof* mutant. Invest Ophthalmol Vis Sci 2007; 48:522-9. [PMID: 17251445].

30. Bodenbender J-P, Marino V, Philipp J, Tropitzsch A, Kernstock C, Stingl K, Kempf M, Haack TB, Zuleger T, Mazzola P, Kohl S, Weisschuh N, Dell'Orco D, Kühlewein L. Comprehensive analysis of two hotspot codons in the TUBB4B gene and associated phenotypes. Sci Rep 2024; 14:10551-[PMID: 38719929].

31. Luscan R, Mechaussier S, Paul A, Tian G, Gérard X, Defoort-Dellhemmes S, Loundon N, Audo I, Bonnin S, LeGargasson JF, Dumont J, Goudin N, Garfa-Traoré M, Bras M, Pouliet A, Bessières B, Boddaert N, Sahel JA, Lyonnet S, Kaplan J, Cowan NJ, Rozet JM, Marlin S, Perrault I. Mutations in TUBB4B Cause a Distinctive Sensorineural Disease. Am J Hum Genet 2017; 101:1006-12. [PMID: 29198720].

32. Nasevicius A, Ekker SC. Effective targeted gene 'knockdown' in zebrafish. Nat Genet 2000; 26:216-20. [PMID: 11017081].

33. Sanzhaeva U, Boyd-Pratt H, Bender PTR, Saravanan T, Rhodes SB, Guan T, Billington N, Boye SE, Cunningham CL, Anderson CT, Ramamurthy V. TUBB4B is essential for the cytoskeletal architecture of cochlear supporting cells and motile cilia development. Commun Biol 2024; 7:1146-[PMID: 39277687].

34. Maasz A, Hadzsiev K, Ripszam R, Zsigmond A, Maka E, Knezy K, Lesch B, Nemeth A, Bene J, Galik B, Gyenesei A, Melegh B. TUBB4B gene mutation in Leber phenotype of congenital amaurosis syndrome associated with early-onset deafness. Eur J Med Genet 2022; 65:104471[PMID: 35240325].

35. McFadden JR, Tolete CDP, Huang Y, Macnamara E, Sept D, Nesterova G, Gahl WA, Sackett DL, Malicdan MCV. Clinical, genetic, and structural characterization of a novel TUBB4B tubulinopathy. Mol Genet Metab Rep 2023; 36:100990[PMID: 37448631].

36. Dodd DO, Mechaussier S, Yeyati PL, McPhie F, Anderson JR, Khoo CJ, Shoemark A, Gupta DK, Attard T, Zariwala MA, Legendre M, Bract D, Wallmeier J, Gui M, Fassad MR, Parry DA, Tennant PA, Meynert A, Wheway G, Fares-Taie L, Black HA, Mitri-Frangieh R, Faucon C, Kaplan J, Patel M, McKie L, Megaw R, Gatsogiannis C, Mohamed MA, Aitken S, Gautier P, Reinholt FR, Hirst RA, O'Callaghan C, Heimdal K, Bottier M, Escudier E, Crowley S, Descartes M, Jabs EW, Amiel J, Bacci GM, Calogero C, Palazzo V, Tiberi L, Blumlein U, Rogers A, Wambach JA, Wegner DJ,

Fulton AB, Kenna M, Rosenfeld M, Holm IA, Quigley A, Hall EA, Murphy LC, Cassidy DM, von Kriegsheim A. Scottish Genomes Partnership, Genomics England Research Consortium, Undiagnosed Diseases Network, Papon J-F, Pasquier L, Murris MS, Chalmers JD, Hogg C, Macleod KA, Urquhart DS, Unger S, Aitman TJ, Amselem S, Leigh MW, Knowles MR, Omran H, Mitchison HM, Brown A, Marsh JA, Welburn JPI, Ti, S-C, Horani A, Rozet J-M, Perrault I, Mill P. Ciliopathy patient variants reveal organelle-specific functions for TUBB4B in axonemal microtubules. Science 2024; 384:404-.

37. Stooke-Vaughan GA, Obholzer ND, Baxendale S, Megason SG, Whitfield TT. Otolith tethering in the zebrafish otic vesicle requires Otogelin and α-Tectorin. Development 2015; 142:1137-45. [PMID: 25758224].

38. Bever MM, Fekete DM. Atlas of the developing inner ear in zebrafish. Dev Dyn 2002; 223:536-43. [PMID: 11921341].

39. Baxendale S, Whitfield TT. Methods to study the development, anatomy, and function of the zebrafish inner ear across the life course. In: Detrich III HW, Westerfield M, Zon LI, editors. Methods in Cell Biology, Vol 134. New York; Elsevier Ltd; 2016. P. 165–209.

40. Sewell MT, Legué E, Liem KF Jr. Tubb4b is required for multi-ciliogenesis in the mouse. Development 2024; 151:201819[PMID: 38031972].

41. el-Amraoui A, Sahly I, Picaud S, Sahel J, Abitbol M, Petit C. Human Usher 1B/mouse shaker-1: the retinal phenotype discrepancy explained by the presence/absence of myosin VIIA in the photoreceptor cells. Hum Mol Genet 1996; 5:1171-8. [PMID: 8842737].

42. Sahly I, Dufour E, Schietroma C, Michel V, Bahloul A, Perfettini I, Pepermans E, Estivalet A, Carette D, Aghaie A, Ebermann I, Lelli A, Iribarne M, Hardelin J-P, Weil D, Sahel J-A, El-Amraoui A, Petit C. Localization of Usher 1 proteins to the photoreceptor calyceal processes, which are absent from mice. J Cell Biol 2012; 199:381-99. [PMID: 23045546].

Articles are provided courtesy of Emory University and The Abraham J. & Phyllis Katz Foundation. The print version of this article was created on 16 May 2025. This reflects all typographical corrections and errata to the article through that date. Details of any changes may be found in the online version of the article.